Alternating Dual-Pulse, Dual-Frequency Techniques for Range and Velocity Ambiguity Mitigation on Weather Radars

SEBASTIÁN TORRES

SMT Consulting, Norman, Oklahoma

RICHARD PASSARELLI JR. AND ALAN SIGGIA

Vaisala, Inc., Westford, Massachusetts

PENTTI KARHUNEN

Vaisala Oyj, Helsinki, Finland

(Manuscript received 13 July 2009, in final form 29 April 2010)

ABSTRACT

This paper introduces a family of alternating dual-pulse, dual-frequency (ADPDF) techniques. These are based on frequency diversity and are proposed as a means to mitigate range and velocity ambiguities on Doppler weather radars. ADPDF techniques are analyzed theoretically and through simulated and real weather data collected with a prototype C-band radar. Analogous to single-frequency, multiple-pulse-repetition-time (mPRT) techniques, such as staggered or triple PRT, it is demonstrated that ADPDF techniques can extend the maximum unambiguous velocity beyond what is achievable with uniform sampling. However, unlike mPRT techniques, ADPDF techniques exhibit better statistical performance and, more importantly, may be designed to preserve uniform sampling on one of the frequency channels, thus avoiding some of the difficulties associated with processing nonuniformly sampled data.

1. Introduction

An intrinsic limitation of pulsed Doppler radars is given by the fact that maximum unambiguous range (r_a) and Doppler velocity (v_a) are inversely coupled. For a weather radar transmitting uniformly spaced pulses, the range–velocity product is given by

$$r_a v_a = \frac{c\lambda}{8}, \tag{1}$$

where c is the speed of light and λ is the radar wavelength (Doviak and Zrnić 1993). It is easy to see from (1) that trying to improve r_a or v_a necessarily results in worsening the other, and trade-offs are often needed that hamper the observation of severe weather phenomena, especially at shorter wavelengths. Fortunately, significant strides have been made in the development of signal-processing techniques that mitigate range and velocity ambiguities on weather radars (e.g., Zrnić and Mahapatra 1985). For example, two complementary techniques—staggered pulse repetition time (PRT) and systematic phase coding—have been suggested and currently are either operational or scheduled for future upgrades of the U.S. Next Generation Weather Radar (NEXRAD) network (Torres 2005, 2006). Although the performance of these techniques has proven to be quite satisfactory on S-band radars, the problem of range and velocity ambiguities on X- and C-band radars is more severe, and more aggressive mitigation approaches are usually demanded. To illustrate this, consider the performance of staggered PRT for the observation of severe storms at different radar wavelengths. Data from tornadic storms compiled by Doviak and Zrnić (1993) exemplify typical radial velocities that can easily span a ± 50 m s^{-1} interval. At S band ($\lambda = 10$ cm), staggered PRT with $T_1 = 1$ ms and $T_2 = 1.5$ ms (i.e., a PRT ratio of $^2/_3$ as recommended for the NEXRAD network) would result in the required v_a of 50 m s^{-1} and would provide an r_a of 225 km (Torres et al. 2004). However, at C and X bands ($\lambda = 5$ and 3 cm, respectively), staggered PRTs producing the same v_a would

Corresponding author address: Sebastián Torres, 3825 Crail Drive, SMT Consulting, Norman, OK 73072.
E-mail: smtorres@ieee.org

DOI: 10.1175/2010JTECHA1355.1

result in shorter r_a of 112 km and a mere 67 km, respectively. Still, the staggered PRT r_a at shorter wavelengths could be improved, for example, by using larger PRT ratios such that the required v_a is achieved with longer PRTs (Zrnić and Mahapatra 1985). However, staggered PRT ratios larger than 2/3 would result in larger errors of velocity estimates and would be less attractive because of the lack of effective ground clutter–filtering techniques.[1]

Although the use of frequency diversity on weather radars is not new, its application for the mitigation of range and velocity ambiguities has been rather limited. Exploiting the concept of frequency diversity, we propose a family of sampling and signal-processing techniques to increase the maximum unambiguous range and velocity product similar to what is achievable with multiple-PRT (mPRT) techniques, such as staggered or triple PRT. However, unlike mPRT techniques, the proposed techniques exhibit better statistical performance and, more importantly, may be designed to preserve uniform sampling on one of the frequency channels, thus avoiding some of the difficulties associated with processing nonuniformly sampled data.

2. Dual-frequency Doppler radar

Doviak et al. (1976) first applied the idea of frequency diversity to mitigate range and velocity ambiguities in what they termed dual-wavelength Doppler radar whereby coherent signals of slightly different frequencies f_1 and f_2 are transmitted simultaneously and mixed at the receiver. They showed that the resulting ''differential'' Doppler shift corresponding to the beat frequency $f_2 - f_1$ is lower than the Doppler shift of either frequency channel, effectively increasing the range of unambiguous velocities. However, the authors questioned the practicality of this approach because of the technological limitations at that time and the fact that simpler techniques, such as staggered PRT, exhibit similar performance in mitigating ambiguities.

Later, Doviak et al. (1979) extended the dual-wavelength Doppler radar concept proposing closely spaced frequencies that are apart enough to ensure uncorrelated channels. They allowed each frequency channel to transmit a different PRT: a long PRT, yielding a large unambiguous range for reflectivity, was proposed for one channel, whereas a short PRT was proposed for velocity estimation on the other channel. This technique is analogous to the (single frequency) ''batch mode'' processing that is currently implemented on NEXRAD, but has the additional advantage of reducing the acquisition time. Later, Glover et al. (1981) reported an implementation of this dual-frequency technique on a proof-of-concept Doppler weather radar for NEXRAD in which, essentially, two radars shared one antenna.

Doviak et al. (1979) also suggested replacing the short PRT with staggered PRT sampling to obtain ''automatic'' velocity dealiasing. However, to our knowledge, the practicality and performance of this idea was neither explored any further nor was it revisited, until now.

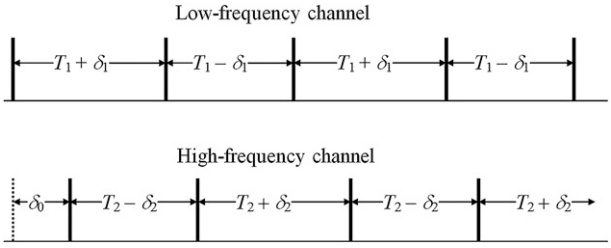

FIG. 1. General ADPDF sampling scheme for the two frequency channels. Times at which a pulse is sent by the radar transmitter(s) is indicated (solid vertical lines).

3. Alternating dual-pulse, dual-frequency techniques

In this work, we introduce a family of alternating dual-pulse, dual-frequency techniques (ADPDF). These are based on frequency diversity and extend the idea of Doviak et al. (1979) to mitigate range and velocity ambiguities on Doppler weather radars.

a. ADPDF sampling

Sampling for the low- and high-frequency channels (denoted by subscripts 1 and 2, respectively) is given in Fig. 1. Here, T_1 and T_2 are termed the ''base'' PRTs, δ_1 and δ_2 (which are much smaller than T_1 and T_2) control PRT staggering on each channel, and δ_0 is the initial time shift between the two frequency channels.

A family of ADPDF techniques can be obtained by selecting sampling parameters in different ways. For example, PRT staggering can be eliminated from either frequency channel (i.e., producing uniform PRT) by setting either δ_1 or δ_2 to zero. Additionally, one of the ''base'' PRTs can be made long enough to eliminate range ambiguities, whereas the other one can be kept short enough to minimize velocity aliasing, as in Doviak et al. (1979). Further, it is possible to use the same transmitter for both channels by choosing T_1 and T_2 carefully (e.g., $T_1 = T_2$) and by increasing δ_0 so that duty cycle requirements are easily met as a result of the balanced interlacing of transmitter pulses. This is a clear advantage

[1] The staggered PRT ground clutter filter proposed for NEXRAD (Sachidananda and Zrnić 2002) meets the NEXRAD technical requirements but was designed for a 2/3 PRT ratio only.

over the two-transmitter design implemented by Glover et al. (1981).

Regardless of the choice of sampling parameters to minimize the occurrence of range and velocity ambiguities, an additional benefit of frequency diversity is the potential reduction in acquisition time by having more samples available in the dwell time. This holds if the two frequencies are spaced by more than the reciprocal of the transmitted pulse width so that the signals from the two frequency channels are uncorrelated (Doviak and Zrnić 1993). Evidently, these benefits come at the following price: 1) increased complexity to control transmitter pulsing, 2) additional hardware to receive signals from two frequency channels, and 3) increased throughput required to process more samples for a given dwell time.

In the next sections, we focus our study on three cases of ADPDF sampling. The first case (ADPDF1) exhibits PRT staggering on both frequency channels, both of which have the same ''base'' PRT; the sampling parameters are $T_1 = T_2 = T$ and $\delta_0 = \delta_1 = \delta_2 = \delta$. The second case (ADPDF2) exhibits uniform PRT on one channel and staggered PRT on the other; the sampling parameters are $T_1 = T_2 = T, \delta_0 = \delta, \delta_1 = 0$, and $\delta_2 = 2\delta$. The last case (ADPDF3) is the same as ADPDF2, except that $\delta_0 = T/2$.

b. ADPDF Doppler velocity estimation

Denote the complex radar signals from the two frequency channels by V_1 and V_2. The numbers of samples in the dwell time for each channel (M_1 and M_2) depend on the ADPDF sampling parameters. In general, M_1 and M_2 are not the same; however, for the three variations under analysis we can assume that $M_1 = M_2 = M$.

Doppler velocity can be typically estimated from the weather signal autocorrelation at any nonzero lag. In the case of ADPDF signals, we could exploit the particular sampling and use multiple readily available lags; instead, let us consider the following interesting quantity:

$$R_{\delta_1+\delta_2} = \frac{1}{M-1}\sum_{m=0}^{M-2} R_{12}(m)R_{12}(m+1), \tag{2}$$

where

$$R_{12}(m) = \begin{cases} V_1^*(m)V_2(m), & m \text{ even} \\ V_1(m)V_2^*(m), & m \text{ odd} \end{cases}; \quad \text{for} \quad m = 0, \ldots, M-1. \tag{3}$$

Note that $R_{\delta_1+\delta_2}$ is *not* the autocorrelation function at lag $\delta_1 + \delta_2$. However, it will be shown that it allows unambiguous Doppler velocity measurements in the same interval as if the autocorrelation at lag $\delta_1 + \delta_2$ was available. After taking the expected value of (2) and splitting the sum into its even and odd terms, using the fact that the signals from the two frequency channels are uncorrelated, it can be proven that

$$E[R_{\delta_1+\delta_2}] = aR_1(T_1+\delta_1)R_2^*(T_2-\delta_2) + bR_1^*(T_1-\delta_1)R_2(T_2+\delta_2), \tag{4}$$

where R_1 and R_2 are the autocorrelation functions for the high- and low-frequency channels, respectively. The real constants a and b are the fraction of summands in (2) corresponding to even and odd values of m, respectively. For odd M, $a = b = 0.5$; however, for even M, $a = 0.5M(M-1)^{-1}$ and $b = 0.5(M-2)(M-1)^{-1}$, which converge to 0.5 as the number of samples becomes large.

With the usual Gaussian assumption for the weather signal spectrum, the autocorrelation functions for any lag t are given by

$$R_i(t) = S_i\rho_i(t)\exp(-j4\pi\bar{v}_i t/\lambda_i), \quad \text{for} \quad i = 1,2, \tag{5}$$

where S is the weather signal power, $\bar{v}$ is the mean Doppler velocity, and

$$\rho_i(t) = \exp[-8(\pi\sigma_{v,i}t/\lambda_i)^2], \tag{6}$$

where σ_v is the spectrum width (Doviak and Zrnić 1993). Further, if the propagation properties of the signal and the scattering properties of the hydrometeors are very similar for both frequency channels (i.e., spectral moments are the same for both frequency channels), it can be shown that the arguments of the two terms on the right-hand side of (4) can be approximated to be the same. That is,

$$\arg[R_1(T_1+\delta_1)R_2^*(T_2-\delta_2)] = -4\pi\bar{v}\left(\frac{T_1+\delta_1}{\lambda_1} - \frac{T_2-\delta_2}{\lambda_2}\right) = -4\pi\bar{v}\frac{(\lambda_2-\lambda_1)T + \lambda_2\delta_1 + \lambda_1\delta_2}{\lambda_1\lambda_2} \approx -4\pi\bar{v}\frac{\lambda_2\delta_1 + \lambda_1\delta_2}{\lambda_1\lambda_2}, \tag{7}$$

and

$$\arg[R_1^*(T_1-\delta_1)R_2(T_2+\delta_2)] = -4\pi\bar{v}\left(-\frac{T_1-\delta_1}{\lambda_1}+\frac{T_2+\delta_2}{\lambda_2}\right) = -4\pi\bar{v}\frac{(\lambda_1-\lambda_2)T+\lambda_2\delta_1+\lambda_1\delta_2}{\lambda_1\lambda_2} \approx -4\pi\bar{v}\frac{\lambda_2\delta_1+\lambda_1\delta_2}{\lambda_1\lambda_2}. \tag{8}$$

These approximations hold because even for the longer typical weather radar wavelengths (~10 cm) and typical transmitter pulse widths (~1 μs), the frequency spacing between the two channels is such that $(\lambda_1 - \lambda_2)$ is at least three orders of magnitude smaller than λ_1 (or λ_2), whereas the proposed values of δ_1 and δ_2 are not more than one order of magnitude smaller than T. Hence, the argument of (4) is independent of a or b and is given by

$$\arg\{E[R_{\delta_1+\delta_2}]\} \approx -4\pi\bar{v}\frac{\lambda_2\delta_1+\lambda_1\delta_2}{\lambda_1\lambda_2}. \tag{9}$$

Finally, the same reasoning can be used to further approximate (9), and using the fact that for the three techniques under analysis $\delta_1 + \delta_2 = 2\delta$,

$$\arg\{E[R_{2\delta}]\} \approx -4\pi\bar{v}\frac{\lambda_2(\delta_1+\delta_2)+(\lambda_1-\lambda_2)\delta_2}{\lambda_1\lambda_2} \approx -8\pi\bar{v}\delta/\lambda_1. \tag{10}$$

Therefore, the mean Doppler velocity can be estimated from the argument of $R_{2\delta}$ as

$$\hat{v} = -\frac{\lambda_1}{8\pi\delta}\arg(R_{2\delta}). \tag{11}$$

Comparing this formula to the classical pulse-pair estimator [e.g., Eq. (6.19) in Doviak and Zrnić 1993], we can see that the outlined processing technique is equivalent to using a uniform PRT of 2δ, a quantity that can be made arbitrarily small without changing the basePRT T that determines the maximum unambiguous range.

c. Mitigation of range and velocity ambiguities

The performance of range and velocity ambiguity mitigation techniques can be characterized using the theoretical maximum unambiguous range–velocity product (RVP). In this section, the RVP for single-frequency mPRT and ADPDF techniques are computed and compared to the standard single-frequency uniform PRT case.

1) SINGLE-FREQUENCY UNIFORM PRT

As given in (1), the single-frequency uniform PRT (UPRT) technique RVP is

$$r_a v_a = \left(\frac{cT}{2}\right)\left(\frac{\lambda}{4T}\right) = \frac{c\lambda}{8}. \tag{12}$$

This quantity can be doubled by employing systematic phase coding of transmitted pulses (Zrnić and Mahapatra 1985). Whereas the maximum unambiguous velocity is still given by the uniform PRT T, the maximum unambiguous range can be increased by a factor of 2 because the algorithm allows the retrieval of Doppler velocities from two overlaid echoes.

2) SINGLE-FREQUENCY STAGGERED PRT

The staggered PRT (SPRT) technique provides the extension of the maximum unambiguous velocity by using two alternating PRTs and computing velocity estimates from autocorrelations at the two available lags. These velocity estimates alias in different Nyquist intervals, and their difference is used to determine their correct Nyquist cointerval. Herein, we consider the performance of the staggered PRT algorithm as described by Torres et al. (2004) whereby a set of dealiasing rules for a PRT ratio of the form $T_1/T_2 = m/n$ is used to extend the maximum unambiguous velocity to $v_a = mv_{a1} = nv_{a2}$, where m and n are positive integers and v_{a1} and v_{a2} are the maximum unambiguous velocities corresponding to the short and long PRT, respectively. With the usual assumption of $T_1 < T_2$, the maximum unambiguous range for velocity measurements is given by $r_a = cT_1/2$ (note that this differs from the maximum unambiguous range for reflectivity measurements given by T_2 that was used in the introduction). Hence, the SPRT RVP is

$$r_a v_a = \left(\frac{cT_1}{2}\right)\left(m\frac{\lambda}{4T_1}\right) = \left(\frac{c\lambda}{8}\right)m, \tag{13}$$

which reveals an improvement by a factor of m over UPRT.

3) SINGLE-FREQUENCY TRIPLE PRT

Analogous to staggered PRT, the triple PRT (TPRT) technique extends the maximum unambiguous velocity by cyclically sampling using three PRTs and computing velocity estimates for each of these three lags. Using the algorithm described by Tabary et al. (2006) for PRT ratios of the form $T_1/T_2 = m/n$ and $T_1/T_3 = p/q$, the maximum unambiguous velocity can be extended as $v_a = \text{lcm}(m, p)v_{a1}$, where lcm is the least common multiple. TPRT velocity dealiasing is accomplished via a "clustering" algorithm. That is, from all possible aliases for the three estimated velocities, the "cluster" that

minimizes the root-mean-square error is used to select the dealiased velocity with the lowest variance. With the usual assumption of $T_1 < T_2 < T_3$, the maximum unambiguous range for velocity measurements is the same as with SPRT and given by $r_a = cT_1/2$. Hence, the TPRT RVP is

$$r_a v_a = \left(\frac{cT_1}{2}\right)\left[\mathrm{lcm}(m, p)\frac{\lambda}{4T_1}\right] = \left(\frac{c\lambda}{8}\right)\mathrm{lcm}(m, p), \quad (14)$$

which indicates an improvement by a factor of $\mathrm{lcm}(m, p)$ over UPRT. Note that $\mathrm{lcm}(m, p) \geq m$; thus, with the proper choice of PRT ratios, the TPRT technique can be designed to have improved performance also relative to SPRT.

4) ADPDF

Strictly speaking, the maximum unambiguous range for ADPDF techniques would be given by the shortest PRT used in each particular sampling scheme. For simplicity, assume that $\delta \ll T$, so that all ADPDF techniques under consideration have approximately the same unambiguous range given by

$$r_a \approx cT/2. \quad (15)$$

As shown by (11), the extended maximum unambiguous velocity with ADPDF is

$$v_a = \lambda_1/8\delta. \quad (16)$$

Hence, the ADPDF RVP is given by

$$r_a v_a = \left(\frac{cT}{2}\right)\left(\frac{\lambda_1}{8\delta}\right) = \left(\frac{c\lambda_1}{8}\right)\left(\frac{T}{2\delta}\right), \quad (17)$$

which reveals an improvement by a factor of $T/2\delta$ over UPRT.

Note that ADPDF, SPRT, and TPRT improvement factors, and hence their corresponding range–velocity products, can be made arbitrarily large by adjusting the ratios of the PRTs in each sampling scheme. However, this adjustment usually comes at a price. For ADPDF, the improvement factor can be arbitrarily increased by reducing the value of δ. However, as shown next, the ratio T/δ also controls the variance of velocity estimates computed from (11).

d. *Performance of the ADPDF Doppler velocity estimator*

A priori, it would appear that ADPDF techniques could be used to arbitrarily increase the range–velocity product. However, another critical measure of performance is given by the variance of the Doppler velocity estimator in (11), which is evaluated next using simulations.

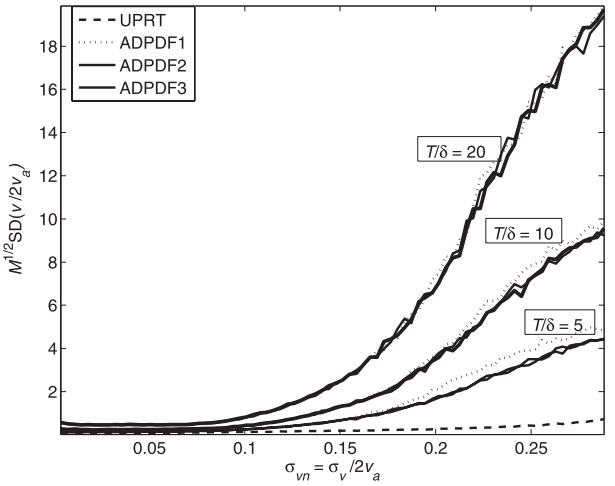

FIG. 2. Normalized standard deviation of velocity estimates vs the normalized spectrum width for standard UPRT and ADPDF1, ADPDF2, and ADPDF3 for different T/δ ratios. The normalizing unambiguous velocity is $v_a^{(\mathrm{UPRT})} = \lambda_1/4T$.

Time series data are simulated using the classical method by Zrnić (1975). For distributed scatterers, if the frequencies from each channel are spaced by more than the inverse of the pulse width (i.e., the Doppler spectra for each frequency channel do not overlap), the underlying random processes for each channel are uncorrelated (Ishimaru 1978). In this case, time series data simulations for each channel can proceed independently. Our simulation assumes that 1) transmission and reception paths are perfectly matched for the two frequency channels, and 2) receiver filters ideally reject out-of-band signals. At first, a very short (uniform) PRT is chosen for both channels. This very short PRT can be computed as the greatest common divisor of δ_0, $T_1 - \delta_1$, $T_1 + \delta_1$, $T_2 - \delta_2$, and $T_2 + \delta_2$ (expressed as integers in any arbitrary units). This allows the simulation of the generalized ADPDF sampling depicted in Fig. 1 by "dropping" appropriate samples.

Figure 2 shows the normalized standard deviation of ADPDF velocity estimates as a function of the normalized spectrum width for high signal-to-noise ratios. Simulations are repeated for a typical range of spectrum widths (0–8 m s^{-1} for $f_1 = 5.4$ GHz and $T = 1$ ms) and three values of T/δ (T is 1 ms and δ is varied to get ratios of 5, 10, and 20). The number of samples is $M = 64$, the SNR is set at 20 dB, and the relative frequency spacing between channels $\Delta f/f_1$ is 0.1% (note that Δf is always larger than the inverse of the pulse width for the frequency bands of interest). For every set of varying parameters, 1000 realizations of time series data are generated. The standard deviation of velocities computed

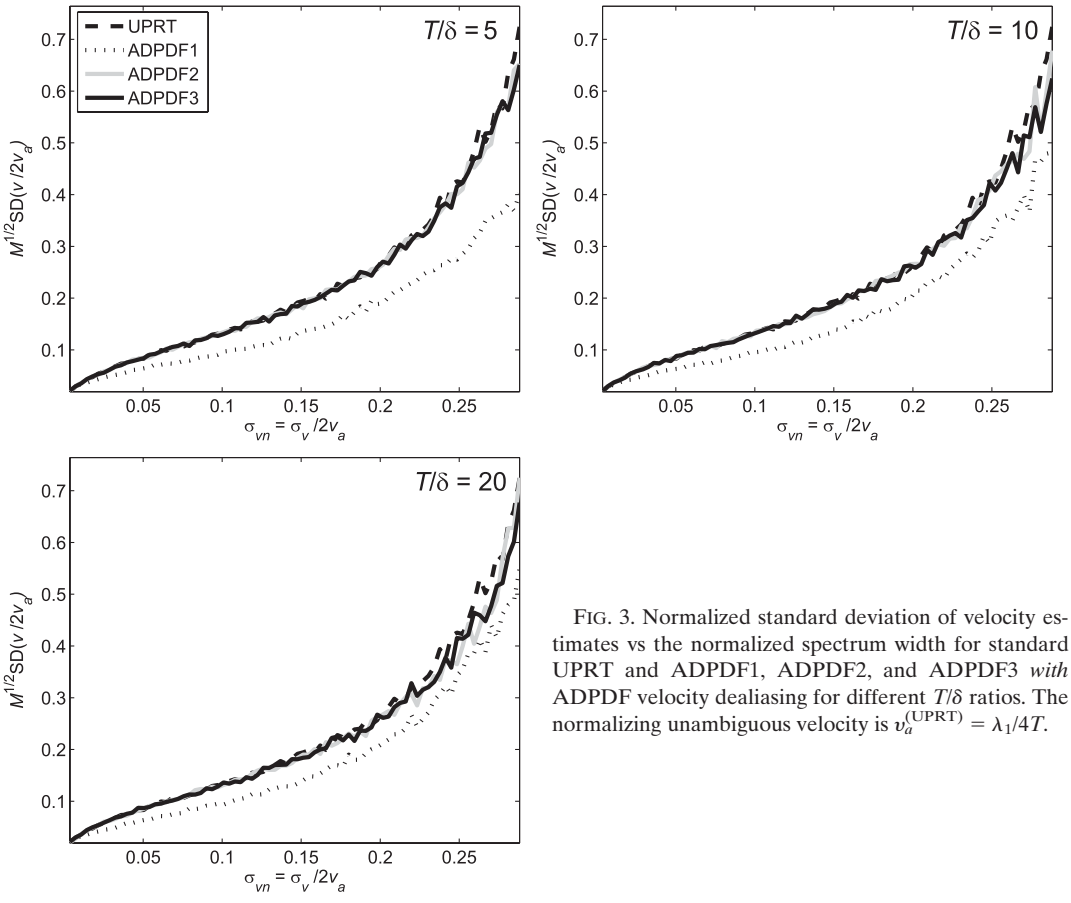

FIG. 3. Normalized standard deviation of velocity estimates vs the normalized spectrum width for standard UPRT and ADPDF1, ADPDF2, and ADPDF3 *with* ADPDF velocity dealiasing for different T/δ ratios. The normalizing unambiguous velocity is $v_a^{(\mathrm{UPRT})} = \lambda_1/4T$.

using single-frequency uniform PRT pulse-pair processing (UPRT) are included for comparison. For generality, standard deviations are normalized by the square root of the number of samples $M^{1/2}$ and UPRT's Nyquist cointerval $2v_a = \lambda_1/2T$. From this figure, it is evident that the standard deviations of ADPDF velocity estimates increase with the T/δ ratio. However, unlike the standard deviation of the UPRT velocity, ADPDF velocity errors grow very rapidly for medium to large spectrum widths, making the estimates impractical in typical operational environments. Because of this, it is not actually feasible to make δ arbitrarily small in order to increase the range–velocity product. Conversely, keeping the standard deviation comparable to UPRT levels requires the use of a small T/δ ratio, effectively limiting the improvement that can be realized through ADPDF. A solution to this apparent dilemma is proposed next.

e. ADPDF velocity dealiasing

ADPDF velocities are unambiguous on a Nyquist interval that is $T/2\delta$ times larger than what is achievable with a uniform PRT T. However, the variances of such velocity estimates increase quite rapidly as the spectrum width increases. Unlike velocity estimates from (11), Doppler velocity estimates from the autocorrelations at lags readily available from either frequency channel (e.g., lag T for ADPDF2) have acceptable errors, but alias into smaller Nyquist intervals. Therefore, the less accurate, nonaliased Doppler velocity estimate from $R_{2\delta}$ (herein referred to as the dealiasing Doppler velocity estimate) can be used to determine the correct Nyquist interval for the more accurate (but likely aliased) Doppler velocity estimate from the autocorrelations at available lags for either channel (herein referred to as the base Doppler velocity estimate). As a result, the dealiased Doppler velocity estimate inherits the errors from the base velocity estimate and the higher errors of the dealiasing velocity can be easily tolerated. Normalized standard deviations of velocity estimates are shown in Fig. 3 for the three ADPDF techniques (with ADPDF velocity dealiasing) as a function of the normalized spectrum width for a high SNR and different values of T/δ (simulation parameters are the same as for Fig. 2). As before, UPRT errors are included as reference. For the three ADPDF techniques, the dealiasing velocity is computed using (11). The base velocity estimate is computed

from $R_1(T-\delta)+R_2(T-\delta)$ for ADPDF1 and from $R_1(T)$ for ADPDF2 and ADPDF3, which among all available lags result in the best statistical performance for each sampling case.

Clearly, ADPDF-dealiased velocity estimates should meet operational requirements because their variances are the same or lower than those obtained with UPRT. This is not entirely surprising because both UPRT velocity estimates and ADPDF base velocity estimates are computed using the classical pulse-pair estimator. In fact, whereas the estimator for ADPDF1 employs more samples, which explains its better performance, the ones for UPRT, ADPDF2, and ADPDF3 are exactly the same. Nevertheless, the standard errors depicted in Fig. 3 do not include dealiasing errors that occur if the base velocity is dealiased into the wrong Nyquist cointerval because of large errors in the dealiasing velocity. These errors are an important component in determining the overall performance of ADPDF techniques and are discussed next.

4. Velocity dealiasing errors with ADPDF techniques

As established in the previous section, compared to UPRT, ADPDF techniques can extend the maximum unambiguous velocity by a factor of $T/2\delta$ while producing velocity estimates with similar statistical performance. However, as with mPRT techniques, ADPDF velocity estimates are vulnerable to dealiasing errors. As the variance of the dealiasing velocity increases, the dealiasing algorithm is more likely to fail. Failure is characterized by the base velocity being dealiased into the wrong Nyquist cointerval; we refer to this as a velocity dealiasing error. The performance of ADPDF techniques is directly tied to the performance of the velocity dealiasing algorithm. Therefore, the velocity dealiasing error rate (VDER) will be used to characterize and compare the performance of ADPDF techniques in a simple and concise manner.

a. ADPDF velocity dealiasing errors

Simulations are repeated with the same parameters used for Figs. 2 and 3. Velocity dealiasing error rates are plotted in Fig. 4 as a function of the normalized spectrum width. Thus, plots are equally applicable to the X-, C-, or S-band radar frequency. The VDER is determined by measuring the percentage of cases for which dealiased velocities depart from the true mean Doppler velocity by more than the maximum unambiguous velocity (smaller departures are assumed to be associated with statistical fluctuations of the base estimate); these are plotted as a function of the normalized spectrum width, where

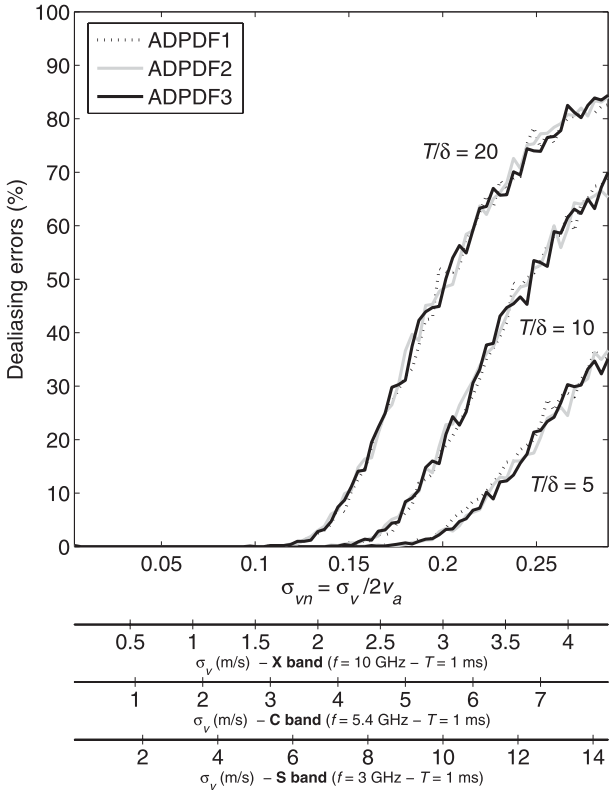

FIG. 4. ADPDF velocity dealiasing error rates vs the normalized spectrum width for the three variations of ADPDF sampling and different T/δ ratios. The normalizing unambiguous velocity is $v_a^{(\mathrm{UPRT})} = \lambda_1/4T$. Spectrum width axes for nominal acquisition parameters at X, C, and S bands are included as a reference.

$v_a^{(\mathrm{UPRT})} = \lambda_1/4T$ is the maximum unambiguous velocity corresponding to UPRT. For reference purposes, spectrum width axes corresponding to $T = 1$ ms and X, C, and S radar frequency bands are included.

Figure 4 shows the performance of ADPDF1, ADPDF2, and ADPDF3 using ADPDF velocity dealiasing (section 3e). Note that the performance is equivalent for all techniques and that it deteriorates with the T/δ ratio. Because the VDER increases with the normalized spectrum width, diminished performance is expected for smaller wavelengths. In other words, because a given normalized spectrum width is about 3 times as large at X band than it is at S band, the performance of ADPDF techniques at X band deteriorates 3 times as quickly as it does for S band.

Because the VDER of ADPDF1, ADPDF2, and ADPDF3 are essentially equivalent, we can choose among these variations based on other considerations. For example, ADPDF2 can be regarded as more attractive than ADPDF1 in the sense that it preserves a uniform PRT on one of the frequency channels. Therefore, it retains the ability to implement signal-processing techniques

that are typically designed to work on uniform PRTs. ADPDF3 could be deemed even more attractive because the selection of δ_0 can be made such that the minimum time between any two transmitted pulses is maximized. Hence, ADPDF3 is better suited for single-transmitter systems with more stringent duty-cycle constraints. In the remainder of this work we focus our analysis on ADPDF3.

b. *Performance comparison with single-frequency mPRT techniques*

Because of the similarities between the ADPDF and mPRT techniques in terms of extension of the maximum unambiguous velocity and their vulnerability to dealiasing errors, it is important to compare their performance before considering the adoption of ADPDF, which requires a more complex radar system. Whereas there are several ways to compare these techniques, a comprehensive study is beyond the scope of this work. Herein, we compare ADPDF3 with ADPDF velocity dealiasing and mPRT techniques that use the same PRTs and result in the same maximum unambiguous range. However, compared to ADPDF, the mPRT techniques might or might not result in the same maximum unambiguous velocity.

Figure 5 shows the normalized standard deviation of velocity estimates and the VDER for ADPDF3, SPRT, and TPRT for different T/δ ratios (simulation parameters are the same as in the previous figures). The single-frequency SPRT sampling alternates between $T - 2\delta$ and T, so the PRT ratios are $3/5$, $4/5$, and $9/10$ for T/δ ratios 5, 10, and 20, respectively. The single-frequency TPRT sampling uses PRTs $T - 2\delta$, T, and $T + 2\delta$, so the PRT ratio pairs are $3/5$ and $3/7$, $4/5$ and $2/3$, and $9/10$ and $9/11$ for T/δ ratios 5, 10, and 20, respectively. Table 1 shows the maximum unambiguous velocities of ADPDF, SPRT, and TPRT for the three T/δ ratios under consideration. For $T/\delta = 5$, SPRT and TPRT have an extended v_a that is twice that of ADPDF3; for $T/\delta = 10$ and 20 all of the techniques result in the same v_a. Still, Fig. 5 shows that for the three T/δ cases, ADPDF3 exhibits similar velocity variances but a larger VDER than either SPRT or TPRT. Hence, although ADPDF3 retains uniform sampling on one of the frequency channels, its applicability might be questionable given than simpler, single-frequency techniques are similarly effective.

5. ADPDF sampling with multiple-PRT processing

As mentioned before, ADPDF sampling is desirable in terms of reducing errors of estimates and preserving uniform PRT sampling while achieving maximum unambiguous velocity extensions at the same level of single-frequency mPRT techniques. However, as shown in the previous section, ADPDF velocity dealiasing error rates are higher than both single-frequency SPRT and TPRT. In this section, we explore combining mPRT processing with ADPDF sampling in an attempt to get the best of both worlds.

Dual-frequency multiple-PRT processing can proceed as in the single-frequency case; that is, by considering velocity estimates from the autocorrelation function at two or more available lags from either frequency channel. The difference between single-frequency and dual-frequency mPRT processing is that autocorrelation pairs are always contiguous (i.e., adjacent pairs share a sample) in the former but may be spaced in the latter.

Next, we consider ADPDF3 sampling with SPRT processing (ADPDF3 + SPRT) that uses autocorrelations $R_2(T - 2\delta)$ and $R_1(T)$ in the same manner as in the single-frequency SPRT technique. These are computed as

$$R_2(T - 2\delta) = \frac{2}{M - 1} \sum_{m=0}^{(M-3)/2} V_2^*(2m) V_2(2m + 1), \quad \text{and} \tag{18}$$

$$R_1(T) = \frac{1}{M - 1} \sum_{m=0}^{M-2} V_1^*(m) V_1(m + 1), \tag{19}$$

where, for convenience, it is assumed that M is odd. Note that unlike with single-frequency SPRT, the short and long PRT autocorrelation pairs are spaced and, more importantly, independent. The autocorrelations in (18) and (19) can be used to estimate short and long PRT mean velocities $\hat{v}_1$ and $\hat{v}_2$ as

$$\hat{v}_1 = -\frac{\lambda_2}{4\pi(T - 2\delta)} \arg[R_2(T - 2\delta)], \quad \text{and} \tag{20}$$

$$\hat{v}_2 = -\frac{\lambda_1}{4\pi T} \arg[R_1(T)]. \tag{21}$$

Thus, the ADPDF3 + SPRT mean velocity estimator $\hat{v}$ is given by

$$\hat{v} = \hat{v}_1 + k \frac{\lambda_2}{2(T - 2\delta)}, \tag{22}$$

where k is the Nyquist interval number obtained from $\hat{v}_1$ and $\hat{v}_2$ using the velocity dealiasing algorithm described by Torres et al. (2004).

Similarly, we consider ADPDF sampling with TPRT processing (ADPDF3 + TPRT) that uses autocorrelations

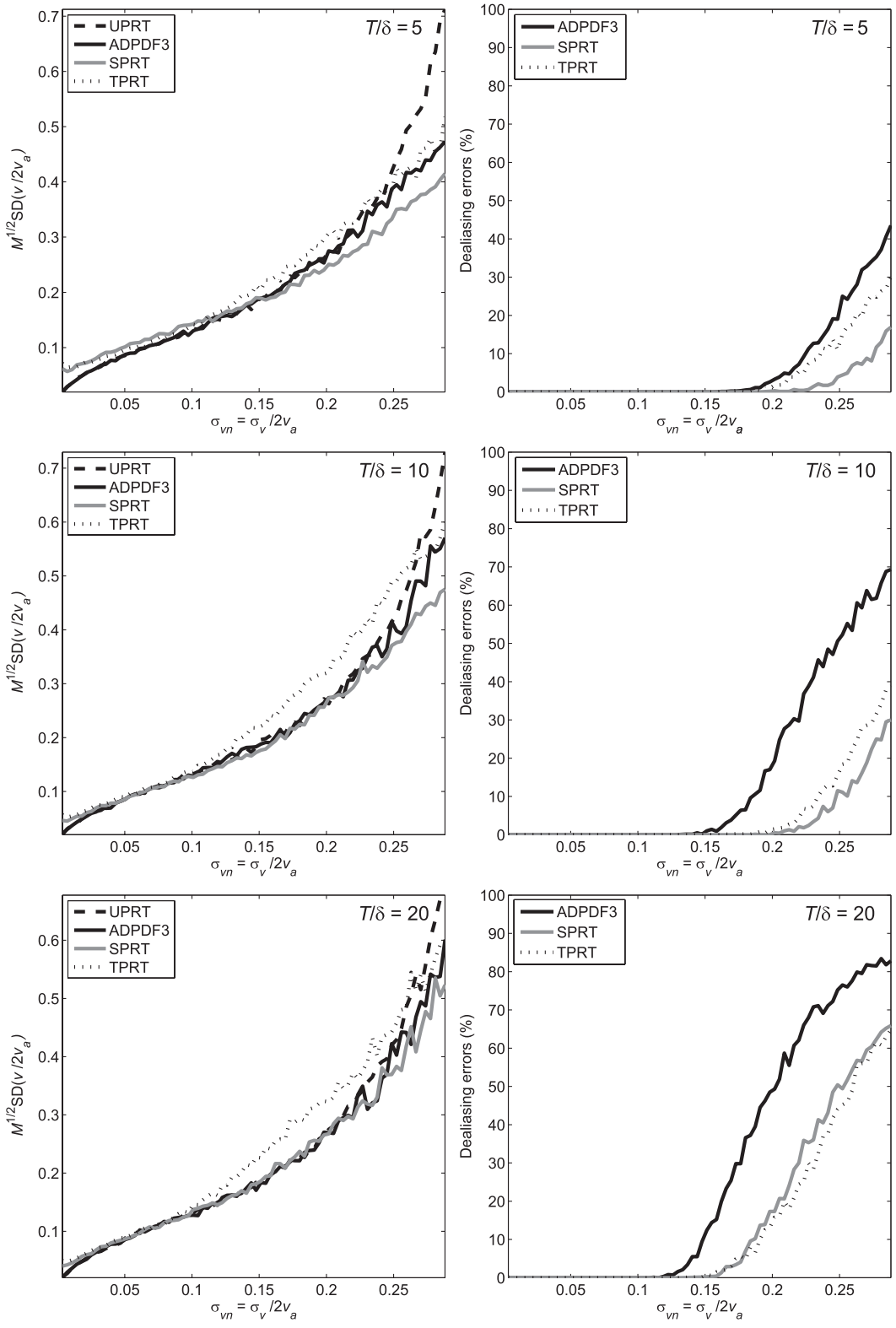

FIG. 5. Normalized standard deviation of (left) velocity estimates and (right) velocity dealiasing error rates vs the normalized spectrum width for ADPDF3 sampling and single-frequency SPRT and TPRT for T/δ ratios of (top) 5, (middle) 10, and (bottom) 20. The normalizing unambiguous velocity is $v_a^{(\mathrm{UPRT})} = \lambda_1/4T$.

TABLE 1. Maximum unambiguous velocities of ADPDF with ADPDF velocity dealiasing and single-frequency SPRT and TPRT techniques as a function of the T/δ ratio.

T/δ \ Technique	ADPDF	SPRT	TPRT
5	$\lambda_1/8\delta$	$\lambda_1/4\delta$	$\lambda_1/4\delta$
10	$\lambda_1/8\delta$	$\lambda_1/8\delta$	$\lambda_1/8\delta$
20	$\lambda_1/8\delta$	$\lambda_1/8\delta$	$\lambda_1/8\delta$

$R_2(T - 2\delta)$, $R_1(T)$, and $R_2(T + 2\delta)$ in the same manner as in the single-frequency TPRT technique. These are computed using (18), (19), and

$$R_2(T + 2\delta) = \frac{2}{M - 1} \sum_{m=0}^{(M-3)/2} V_2^*(2m + 1)V_2(2m + 2), \tag{23}$$

respectively. In this case, $R_2(T - 2\delta)$ and $R_2(T + 2\delta)$ come from contiguous pairs that are independent from the $R_1(T)$ pairs. The short and medium PRT mean velocity estimators ($\hat{v}_1$ and $\hat{v}_2$) are given in (20) and (21); the long-PRT mean velocity $\hat{v}_3$ is estimated as

$$\hat{v}_3 = -\frac{\lambda_2}{4\pi(T + 2\delta)} \arg[R_2(T + 2\delta)]. \tag{24}$$

As in the case of ADPDF3 + SPRT, the ADPDF3 + TPRT mean velocity estimator is given by (22). However, in the TPRT case, k is the Nyquist interval number corresponding to the most consistent velocity triplet when considering all possible aliases of $\hat{v}_1$, $\hat{v}_2$, and $\hat{v}_3$ (Tabary et al. 2006).

Figure 6 shows the normalized standard deviation of velocity estimates and VDER for ADPDF3 with SPRT, and TPRT processing and single-frequency SPRT and TPRT for different T/δ ratios (simulation parameters are the same as in the previous figures). For all T/δ ratios, all techniques lead to the same v_a, but ADPDF3 sampling results in a similar or smaller variance of velocity estimates and lower VDER compared to single-frequency SPRT and TPRT. For $T/\delta = 5$, ADPDF3 + SPRT processing provides the best performance (lowest VDER and velocity variance). For this T/δ ratio, the SPRT ratio is $(T - 2\delta)/T = 3/5$ and the Nyquist velocity is extended to $\lambda_1/4\delta$; that is, twice the value achieved by the ADPDF dealiasing velocity processing discussed in section 3e. For $T/\delta = 10$, ADPDF3 + SPRT and ADPDF3 + TPRT provide similar optimum performance in terms of VDER (but only marginally better than SPRT), but ADPDF3 + SPRT has the edge because it exhibits a slightly lower velocity variance. Finally, for $T/\delta = 20$, ADPDF3 + TPRT is the best option in terms of VDER, but ADPDF3 + SPRT has the lowest velocity variance.

Assuming that the maximum tolerable rate of velocity dealiasing errors is 10% (in practice, this number would depend on the effectiveness of other velocity dealiasing methods, such as techniques based on spatial continuity) and a minimum tolerable rate of SNR is 20 dB, the maximum spectrum widths that limit the usability of these techniques for X band ($f_1 = 10$ GHz) are given in Table 2 (conversion to another frequency f is straightforward by scaling the values on the table with 10 GHz/f). Even though different applications may have different requirements in terms of the range of spectrum widths expected to be measured, it is interesting to put the numbers from Table 2 in an operational context. Fang et al. (2004) provided spectrum width statistics for many weather phenomena; their findings indicate that, on average, the vast majority of weather phenomena have median spectrum widths less than about 2 m s^{-1}. However, for the most severe weather cases, such as convective cores of squall lines, the median spectrum widths are between 4 and 5.4 m s^{-1}. Hence, it is possible to argue that the acceptable performance of ADPDF3 with mPRT processing might be feasible at S and C bands, but only for the smaller T/δ ratios at X band. Nevertheless, the improvement from ADPDF techniques with respect to their single-frequency counterparts in terms of the maximum usable range of spectrum widths is at most ~10%. Note, however, that the performance of mPRT processing may not vary "smoothly" with the T/δ ratio because it depends on the actual PRT ratios.

It is concluded from this analysis that the ADPDF velocity dealiasing process that combines time series from the two frequency channels as in (11) always leads to suboptimal performance. Better performance in terms of VDER and extended Nyquist velocity is always possible if the time series from the two frequency channels are processed independently and multiple-PRT techniques, such as SPRT and TPRT, are exploited.

6. Experimental evaluation of ADPDF techniques

ADPDF3 data were collected on 25 January 2008 with the Vaisala prototype single-transmitter C-band radar located on the Kumpula campus of the University of Helsinki, Finland (Puhakka et al. 2004). On this day, the soundings showed persistent westerly winds of 10–15 m s^{-1} at a height of 1 km. Several sets of time series data were collected with an experimental radar configuration that enabled ADPDF sampling with transmitter frequencies of $f_1 = 5607.6$ MHz and $f_2 = 5603.6$ MHz. Table 3 lists the acquisition parameters for the six cases under analysis. Cases 1 through 3 were collected with a stationary antenna. These cases are useful to compute statistics in order to validate the simulation results in the

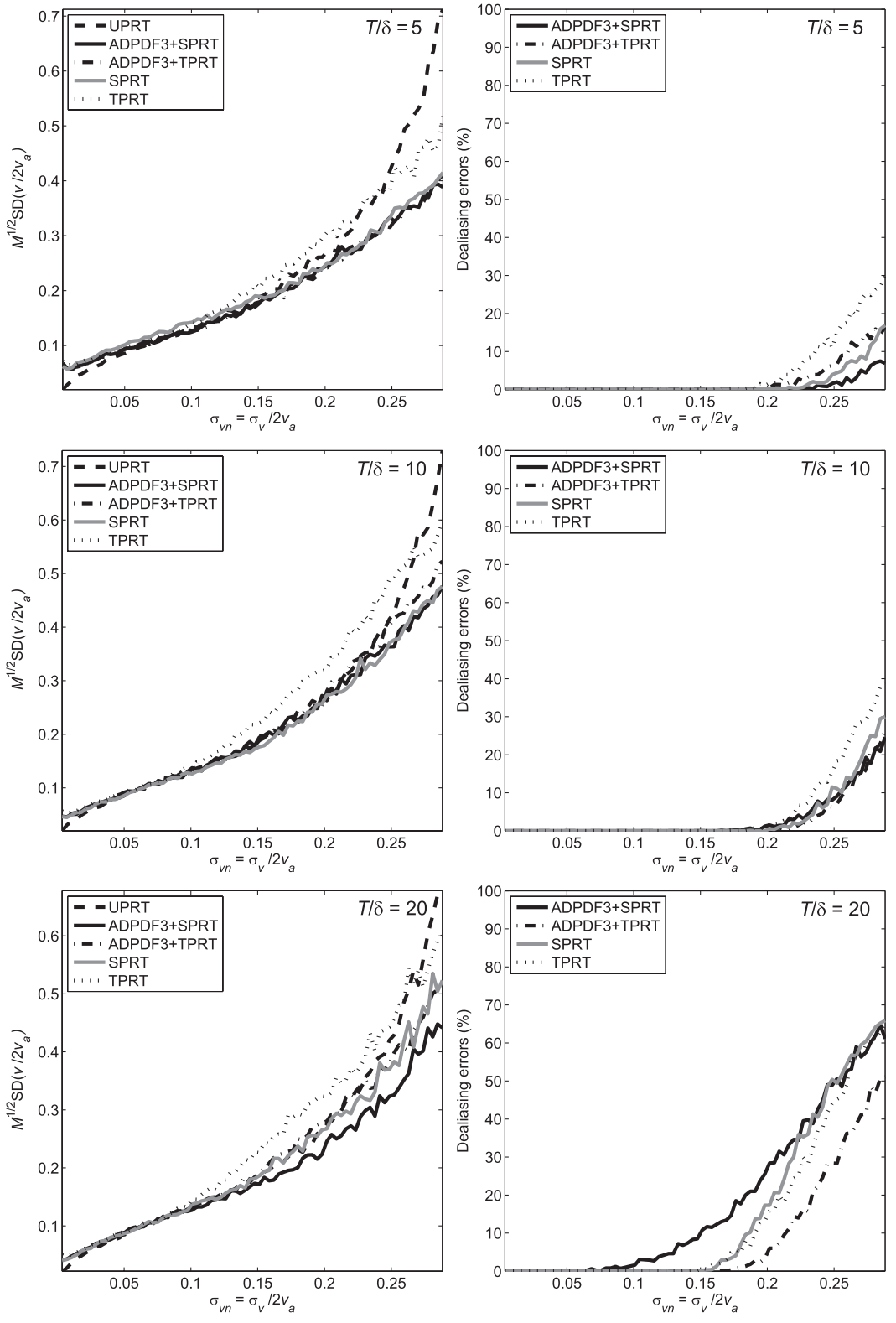

FIG. 6. Normalized standard deviation of (left) velocity estimates and (right) velocity dealiasing error rates vs the normalized spectrum width for ADPDF3 sampling using the SPRT and TPRT processing techniques for velocity dealiasing (ADPDF3 + SPRT and ADPDF3 + TPRT) and single-frequency SPRT and TPRT for T/δ ratios of (top) 5, (middle) 10, and (bottom) 20. The normalizing unambiguous velocity is $v_a^{(\mathrm{UPRT})} = \lambda_1/4T$.

TABLE 2. Approximate maximum spectrum widths, $\sigma_{v,\max}$ (m s^{-1}), that yield maximum velocity dealiasing error rates of 10% for ADPDF techniques with SPRT and TPRT processing and single-frequency SPRT and TPRT techniques for typical X-band radar frequency of 10 GHz as a function of the T/δ ratio for $T = 1$ ms. Values of the best performing techniques are highlighted in bold.

T/δ \ Technique	SPRT	TPRT	ADPDF3 + SPRT	ADPDF3 + TPRT
5	4.10	3.56	**4.42**	3.95
10	3.77	3.52	3.80	**3.88**
20	2.78	2.87	2.28	**3.18**

previous sections. Cases 4 through 6 were collected with a constant-elevation scanning antenna. These were used to assess the overall improvement gained by using ADPDF techniques qualitatively. The three cases in each set have the same uniform PRT ($T = 2$ ms) and T/δ ratios of 5, 10, and 20, respectively.

a. Statistical analysis

Cases 1, 2, and 3 were processed using dual-frequency SPRT (ADPDF3 + SPRT). Because ground clutter filtering was not implemented, gates close to the radar with ground clutter contamination were excluded from the statistical analysis. Furthermore, because spectrum width estimates are greatly affected by noise, gates with an SNR less than 20 dB were also excluded. Finally, for longer PRTs, spectrum width estimates saturate (Melnikov and Zrnić 2004); hence, these were also excluded from the statistical analysis.

Figure 7 shows the rate of VDER for simulated and real ADPDF3 + SPRT velocity estimates as a function of the spectrum width for high SNRs. Velocity dealiasing errors for real data estimates were computed by using the median velocity of all gates with a given spectrum width as the "true" velocity. A dealiasing error was identified if an estimated velocity departed from the median by more than the maximum unambiguous velocity. Although the full range of spectrum widths required for a complete validation is not covered by the real data, the agreement between the real data and the simulations is remarkable.

b. Qualitative analysis

Cases 4, 5, and 6 were processed using dual-frequency SPRT (ADPDF3 + SPRT) and uniform PRT processing (using data just from the high-frequency channel.) Figure 8 shows the reflectivity, UPRT velocity, and ADPDF velocity fields.

Note that the isolation between the frequency channels was not ideal, and leakage from one frequency channel into the other was evident from rings of elevated reflectivities and noisy Doppler velocities (e.g., at about 45 km on case 4). Still, these rings do not appear at the predicted range of $c\delta_0/2$ because, due to the experimental nature of the radar configuration, the two frequency channels could not be maintained in perfect alignment, which resulted in a slow temporal drift for δ_0. However, these were not severe limitations for these proof-of-concept experiments because the value of δ_0 has no bearing on the performance of ADPDF techniques, its value drifted very slowly, and the range gates with power leakage could be easily identified and ignored.

As predicted by the simulations, a small number of dealiasing errors are to be expected when processing time series data using mPRT techniques. These appear as speckles in the velocity field and can be easily identified and corrected. The ADPDF velocity data were postprocessed using a basic velocity dealiasing algorithm based on spatial continuity of the velocity field, which works best when dealing with spatially isolated aliasing problems. This algorithm uses a 7-by-7 gate mask to dealias the central gate based on the median velocity of the remaining gates. Note that the central gate is not replaced (or filtered) by the median velocity of the other gates in the mask. Actually, the best dealiasing for the central gate is chosen to maximize spatial continuity. Figure 8 shows that, unlike for cases processed using ADPDF, all cases processed using single-channel UPRT show significant velocity aliasing (i.e., sharp spatial transitions between bright reds and bright greens).

TABLE 3. Summary of acquisition parameters for the ADPDF3 cases of real data collected with the Kumpula radar. The UPRT and ADPDF3 + SPRT maximum unambiguous velocities are denoted by $v_a^{(\mathrm{UPRT})}$ and v_a, respectively.

Case No.	Azimuth (°)	Elev (°)	T (μs)	δ (μs)	T/δ	$v_a^{(\mathrm{UPRT})}$ (m s^{-1})	v_a (m s^{-1})	M	No. of dwells
1	212	0.9	2000	400	5	6.7	16.7	64	700
2	45	1.5	2000	200	10	6.7	33.4	64	690
3	45	1.5	2000	100	20	6.7	66.8	64	650
4	PPI	0.7	2000	400	5	6.7	16.7	128	330
5	PPI	1.5	2000	200	10	6.7	33.4	128	360
6	PPI	1.5	2000	100	20	6.7	66.8	128	360

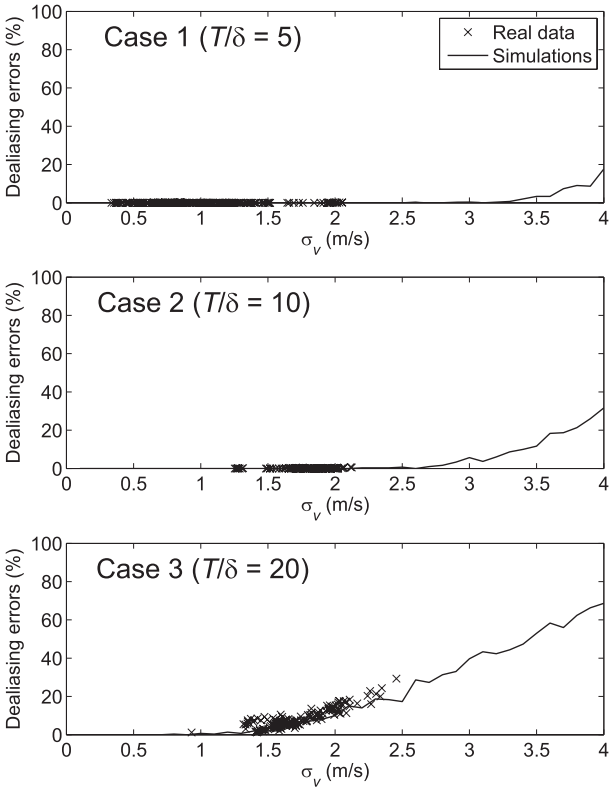

FIG. 7. Simulated and real data velocity dealiasing error rates vs the spectrum width for high SNR. ADPDF data cases (top) 1, (middle) 2, and (bottom) 3 where processed with dual-frequency SPRT (ADPDF3 + SPRT).

7. Conclusions

This paper described a family of range and velocity ambiguity mitigation techniques. These are termed alternating dual pulse, dual frequency (ADPDF) because they exploit frequency diversity in conjunction with sampling and signal-processing strategies to improve the maximum unambiguous range and velocity that can be achieved with uniform sampling.

Whereas sampling schemes that use uniform pulse repetition times are attractive for signal-processing techniques that operate on the Doppler spectrum (e.g., spectral ground clutter filters); they are limited in terms of range and velocity ambiguity mitigation. Random and systematic phase-coding techniques can be used to separate overlaid echoes in the spectral domain, thereby extending the range–velocity product by a factor of 2 while keeping a uniform PRT sampling. In case this performance is insufficient to satisfy operational needs, additional improvement can be obtained with multiple-PRT sampling schemes (e.g., staggered PRT or triple PRT). These techniques can provide significant extension of the maximum unambiguous velocity by adjusting the PRT ratio(s), and therefore result in much larger range–velocity products. Unfortunately, the nonuniform sampling makes the application of classical spectral analysis techniques a challenge.

ADPDF techniques can realize the benefits of both worlds by using frequency diversity. Because they are based on the same theory as the single-frequency multiple-PRT techniques, they have the same extended range–velocity products. However, a significant operational advantage is that ADPDF techniques do not necessarily exclude the implementation of signal-processing techniques that rely on spectral processing because one of the frequency channels can maintain a uniform PRT. Additionally, because samples from the two frequency channels are uncorrelated, it is possible to reduce the acquisition time and/or obtain estimates with lower variance. The additional system complexity required to implement ADPDF techniques can be alleviated by the possibility of sharing one transmitter by interlacing the transmitted pulses for the two frequency channels in a harmonious way. That is, the time between pulses can be maximized without affecting the performance of these techniques to mitigate range and velocity ambiguities.

In principle, the range–velocity product obtained with ADPDF techniques can be made arbitrarily large by reducing the value of δ. However, the main tradeoff for these techniques is given by the rate of velocity dealiasing errors versus the extended maximum unambiguous velocity. That is, larger T/δ ratios do result in larger range–velocity products but lead to higher rates of velocity dealiasing errors, and these errors limit the applicability of ADPDF techniques. The optimum T/δ ratio and processing should be determined based on the radar frequency and the performance of additional velocity dealiasing techniques (e.g., based on spatial continuity), which are implemented down the signal-processing chain. For example, ADPDF3 sampling with $T/\delta = 5$ and SPRT processing seems like a good candidate for all frequency bands. It results in the same velocity variances and extension of the maximum unambiguous velocity as with single-frequency SPRT, but leads to lower velocity dealiasing error rates.

Analyses of several cases of real ADPDF data were used to successfully validate the simulation results and establish the operational feasibility of these techniques. In spite of the limitations of real data, the agreement between real data and simulation results was found to be remarkable. For weather radars that are capable of frequency diversity, ADPDF techniques could significantly improve the mitigation of range and velocity ambiguities, similarly to single-frequency multiple-PRT

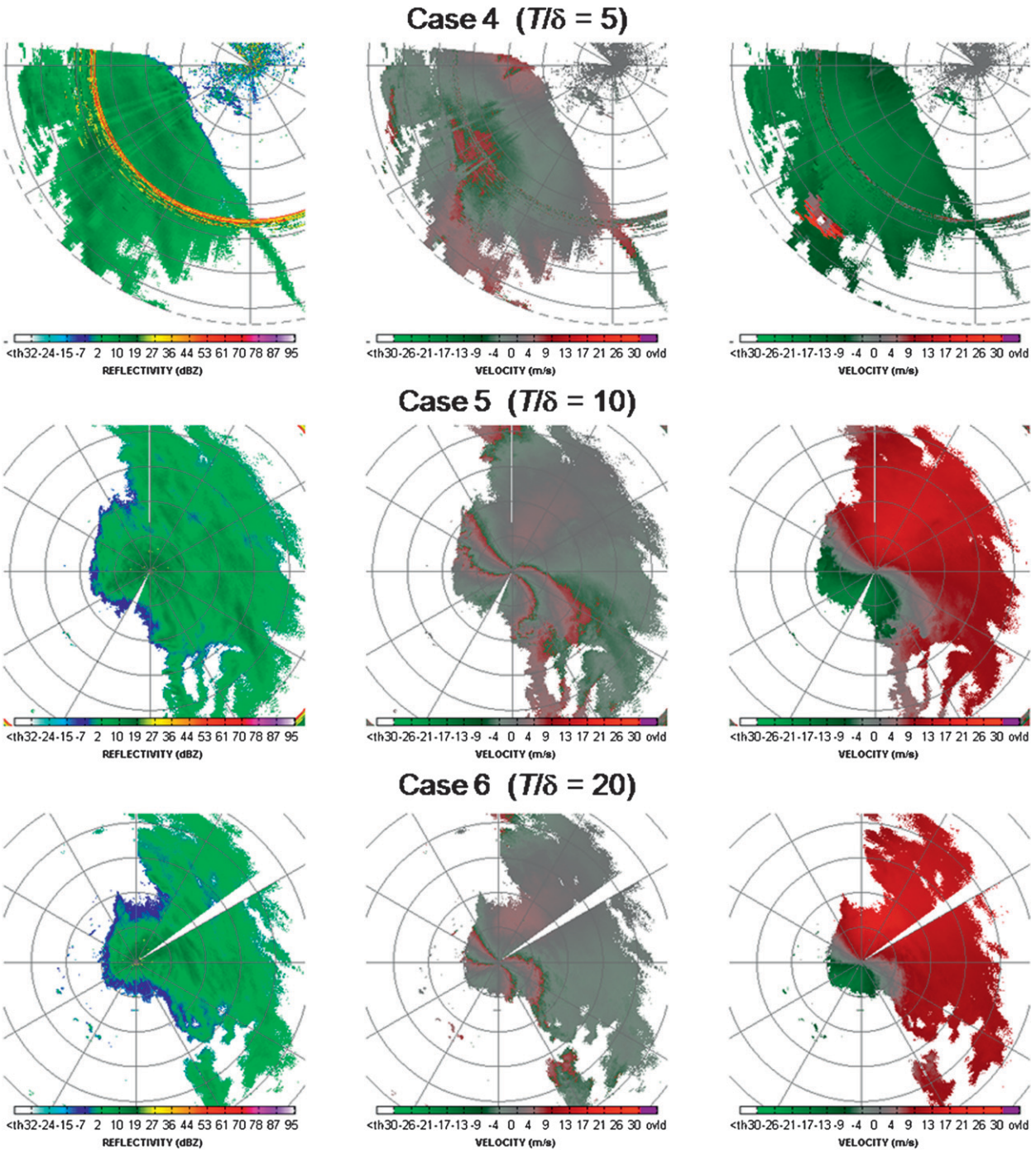

FIG. 8. PPI fields of (left) reflectivity, (middle) uniform PRT velocity, and (right) ADPDF velocity for real data cases (top) 4, (middle) 5, and (bottom) 6 collected with an experimental setting of the C-band Kumpula radar prototype. Range rings are 10 km apart.

techniques, but without the difficulties associated with processing nonuniformly sampled signals.

Acknowledgments. The authors thank two anonymous reviewers for their very useful comments, which helped improve the quality of this manuscript. Also, we are grateful to Reino Keränen for designing and arranging the special ADPDF configuration at the Kumpula radar, and for collecting, organizing, and archiving the real data cases used in this study.

REFERENCES

Doviak, R., and D. Zrnić, 1993: *Doppler Radar and Weather Observations*. Academic Press, 576 pp.

——, D. Sirmans, D. Zrnić, and G. Walker, 1976: Resolution of pulse-Doppler radar range and velocity ambiguities in severe storms. Preprints, *17th Conf. on Radar Meteorology,* Seattle, WA, Amer. Meteor. Soc., 15–22.

——, D. Zrnić, and D. Sirmans, 1979: Doppler weather radar. *Proc. IEEE,* **67,** 1522–1553.

Fang, M., R. J. Doviak, and V. Melnikov, 2004: Spectrum width measured by WSR-88D: Error sources and statistics of various weather phenomena. *J. Atmos. Oceanic Technol.,* **21,** 888–904.

Glover, K. M., G. M. Armstrong, A. W. Bishop, and K. J. Banis, 1981: A dual frequency 10-cm Doppler weather radar. Preprints, *20th Conf. on Radar Meteorology,* Boston, MA, Amer. Meteor. Soc., 738–743.

Ishimaru, A., 1978: *Wave Propagation and Scattering in Random Media*. Vol. 2, Academic Press, 572 pp.

Melnikov, V., and D. Zrnić, 2004: Estimates of large spectrum width from autocovariances. *J. Atmos. Oceanic Technol.,* **21,** 969–974.

Puhakka, T., P. Puhakka, and F. O'Hora, 2004: On the performance of NLFM pulse compression with polarimetric Doppler radar. Preprints, *Fourth European Conf. on Radar in Meteorology and Hydrology (ERAD),* Barcelona, Spain, Copernicus GmbH, 88–91.

Sachidananda, M., and D. S. Zrnić, 2002: An improved clutter filtering and spectral moment estimation algorithm for staggered PRT sequences. *J. Atmos. Oceanic Technol.,* **19,** 2009–2019.

Tabary, P., F. Guibert, L. Perier, and J. Parent-du-Chatelet, 2006: An operational triple-PRT Doppler scheme for the French radar network. *J. Atmos. Oceanic Technol.,* **23,** 1645–1656.

Torres, S., 2005: Range and velocity ambiguity mitigation on the WSR-88D: Performance of the SZ-2 phase coding algorithm. Preprints, *21st Int. Conf. on IIPS for Meteorology, Oceanography, and Hydrology,* San Diego, CA, Amer. Meteor. Soc., 19.2. [Available online at http://ams.confex.com/ams/pdfpapers/83946.pdf.]

——, 2006: Range and velocity ambiguity mitigation on the WSR-88D: Performance of the staggered PRT algorithm. Preprints, *22nd Int. Conf. on IIPS for Meteorology, Oceanography, and Hydrology,* Atlanta, GA, Amer. Meteor. Soc., 9.9. [Available online at http://ams.confex.com/ams/pdfpapers/103695.pdf.]

——, Y. Dubel, and D. S. Zrnić, 2004: Design, implementation, and demonstration of a staggered PRT algorithm for the WSR-88D. *J. Atmos. Oceanic Technol.,* **21,** 1389–1399.

Zrnić, D., 1975: Simulation of weatherlike Doppler spectra and signals. *J. Appl. Meteor.,* **14,** 619–620.

——, and P. Mahapatra, 1985: Two methods of ambiguity resolution in pulse Doppler weather radars. *IEEE Trans. Aerosp. Electron. Syst.,* **21,** 470–483.